

# **Geophysical Studies of Aseismic Ridges in Northern Indian Ocean- Crustal Structure and Isostatic Models**

*Thesis Submitted to the Goa University for the Degree of*

**Doctor of Philosophy**  
*in*  
**Marine Science**



*by*  
**Sreejith K.M.**

**National Institute of Oceanography (CSIR)**

Dona Paula, Goa - 403004, India

*and*

**Space Applications Centre (ISRO)**

Ahmedabad, Gujarat - 380015, India

March 2011

*Dedicated to.....*

*My Achan and Amma*

## **Statement**

As required under the University Ordinance 0.19.8 (vi), I state that the present thesis entitled “**Geophysical Studies of Aseismic Ridges in Northern Indian Ocean-Crustal Structure and Isostatic Models**” is my original research work carried out at the National Institute of Oceanography, Goa and Space Applications Centre, Indian Space Research Organization, Ahmedabad, and that no part thereof has been submitted for any other degree or diploma in any university or institution. The literature related to the problem investigated has been cited. Due acknowledgements have been made wherever facilities and suggestions have been availed of.

**Sreejith K. M.**

Space Applications Centre  
Indian Space Research Organization  
Ahmedabad-380 015

## **Certificate**

This is to certify that the thesis entitled “**Geophysical Studies of Aseismic Ridges in Northern Indian Ocean-Crustal Structure and Isostatic Models**” submitted by **Sreejith K. M.** for the award of the degree of Doctor of Philosophy in the Department of Marine Sciences is based on his original studies carried out by him under my supervision. The thesis or any part thereof has not been previously submitted for any degree or diploma in any university or institution.

**Dr. K. S. Krishna, FASc, FNASc**

Scientist G

National Institute of Oceanography

Council of Scientific and Industrial Research

Dona Paula, Goa- 403 004

## *Acknowledgements*

I hereby express my heartfelt gratitude to my research supervisor Dr. K. S. Krishna, Scientist G, National Institute of Oceanography (NIO), Goa for his inspiring guidance and constant encouragements throughout research work. I am also greatly indebted to Dr. Krishna for introducing me to outstanding geophysical problems related to evolution of major aseismic ridges of the Indian Ocean and plume-oceanic lithosphere interactions, for scientific discussions and for critical comments. It would not have been possible to complete this research work with out his constant motivation and support during the course of work both at NIO, Goa and SAC, Ahmedabad.

I am grateful to Prof. M. Radhakrishna, Department of Earth Science, Indian Institute of Technology, Mumbai (IIT-B) for his valuable guidance for development of process oriented modeling technique and for lengthy scientific discussions which I had for many weekends at IIT-B. I am also thankful to Dr. A. R. Bansal, National Geophysical Research Institute (NGRI) for his support in developing admittance analysis technique.

I thank Council of Scientific and Industrial Research (CSIR), New Delhi for awarding NET-JRF for carrying out research at NIO, Goa. This work is a part of major scientific project that was supported by Department of Science & Technology, New Delhi (project: ESS/16/174/2002) and Indian Space Research Organization (Meteorology and Oceanography Program-II).

I am also grateful to Prof. G. N. Nayak, Co-guide, Department of Marine Science, Goa University for his valuable comments and instructions from time to time. I thank Dr A. K. Chaubey, NIO for his critical reviews and constructive suggestions at various stages of the work. I further thank Dr. T. J. Majumdar, SAC; Dr. Gopala Rao, Osmania University; Dr. K Srinivas, NIO; and Prof. H. B. Menon, Goa University for their discussions and for providing critical comments.

I thankfully acknowledge Dr. S. R. Shetye, Director, NIO for his encouragement and support. I am grateful to Dr. R. R. Navalgund, Director, SAC, for kindly permitting me to continue the Ph.D while working in SAC. I am also grateful to Dr. J. S. Parihar, Deputy Director, EPSA, Dr. Ajai, Group Director, MPSG and Dr. A. S. Rajawat, Head, Geosciences Division for their constant support and encouragement during the course of work at SAC.

I express my sincere thanks to all of my colleagues and friends at NIO for their support and encouragements. From the long list, I may mention the names of Laju, Ajay, Yatheesh, Dileep, Shyju, Jayanth, Shyam, Abu, Pradnya, Sudheesh, Anoop, Nuncio, Sudheesh *chettan*, Rajani, Manoj, Sreekumar, Sijin, Vineesh and Nisha. I specially thank Honey for sending research papers, fruitful scientific discussions and helping me a lot in university matters. I also thank Praveen and Twinkle, IIT-B for their help and support during my visits to IIT-B.

My colleagues at SAC have given me immense support for successful completion of the work. Thanks to Arvind, Phani, Ratheesh, Satadru, Megha, Veera, Ami, Guneswar, Manik, Vanya, Sharad, Sriram and all other lab mates. My SAC friends and football team mates (Dr. Pal, Jidesh, Saji, Bikas, Kaushik, Rakesh, Anoop, Naveen, Ravish, etc.) kept me sane during the course of the work. I specially thank Rajesh *Chettan*, Kamala *Chechi*, Ammu and Appu for their hospitality and encouragements.

I am, indeed, short of words to express my inner-feel to my beloved family members. My father and mother always stood behind me for all important decisions, particularly for pursuing PhD after the Masters Degree. I am highly obliged to my parents for giving me constant encouragements and moral support through out the course of work. Therefore, I dedicate this thesis to them.

## PREFACE

The Indian Ocean is youngest in age and smallest in area relative to the other major oceans, Atlantic and Pacific Oceans. But its structure and evolution are very complex and the ocean encompasses with almost all varieties of geological processes. The structural framework of the northeastern Indian Ocean is unique as the region includes numerous oceanic fracture zones, aseismic ridges, seamounts, abandoned spreading centers, Sunda subduction zone, etc. Besides, the ocean floor is carpeted by enormously thick pre- and post- continental collision sediments discharged from the rivers of east coast of India and Ganges and Brahmaputra. Three aseismic ridges: 85°E Ridge, Ninetyeast Ridge and Comorin Ridge and other major features of the northeastern Indian Ocean have largely contributed in shaping the oceanic and sedimentary basins in the region. It is generally accepted that the Ninetyeast Ridge was formed by the Kerguelen hotspot activity during the rapid northward drift of Indian Plate over the hotspot. Whereas in the case of 85°E Ridge, varied opinions do exist for the evolution of the ridge. The Comorin Ridge is one of the least studied aseismic ridges in the Indian Ocean, thus not much details are available particularly regarding its origin.

The present research work consists of detailed geophysical study of the structure and isostatic compensation mechanisms of the Comorin, Ninetyeast and 85°E ridges. Available ship-borne bathymetry, gravity and magnetic data of the northeastern Indian Ocean extracted from National Geophysical Data Centre (NGDC), are collated with gravity and seismic reflection data generated in various Indian and Russian cruises. The composite geophysical datasets are investigated in detail. The isostasy of the Comorin and Ninetyeast ridges are examined using admittance analysis and two-dimensional gravity forward modeling. In the case of 85°E Ridge, a process oriented modeling technique using seismic and gravity anomaly data was performed as the ridge structure was completely buried under the Bengal Fan sediments. The present research work revealed detailed crustal architecture, isostatic compensation mechanisms and evolutionary models for these three

important aseismic ridges of the northeastern Indian Ocean, thereby the studies have provided new insights to the understanding of the geodynamic evolution of the region.

The thesis comprises seven chapters. A brief description of each chapter is given below:

**Chapter 1** gives an introduction to the concepts of plate tectonics, mantle plumes and isostasy. Some of these basic theories related to the Earth's internal processes are discussed in greater detail as they were extensively used in explaining the evolutionary models of the aseismic ridges. Further, the major objectives of the research work are also described.

**Chapter 2** outlines the structural evolution of the Indian Ocean. A general account of the major aseismic ridges of the Indian Ocean is also described using the up-to-date available geological and geophysical results.

**Chapter 3** describes theoretical and computational aspects of elastic plate model, admittance analysis, backstripping, process oriented gravity modeling and two-dimensional gravity forward modeling. Details of geophysical data sets used in this work are also included.

**Chapter 4** deals with the admittance analysis and forward modeling of gravity and bathymetry data of the Comorin Ridge. Airy model or local compensation with an elastic plate thickness ( $T_e$ ) of about 3 km and crust thickness ( $t$ ) of 15-20 km are suggested for the southern part of the Comorin Ridge (south of  $5^\circ\text{N}$ ), whereas for the northern part a flexural plate model with an elastic thickness of about 15 km is obtained. Admittance analysis together with the results from gravity forward modeling reveal that the south part was emplaced on relatively weak oceanic crust with both surface and sub-surface loading, while the north part was emplaced on the continental crust. For the first time, an attempt has been made to demarcate the Continent-Ocean Boundary on west of Sri Lanka and southern tip of India. The present studies coupled with published plate kinematic models suggested that the Comorin Ridge may have evolved at about 90 Ma during the rift-phase



of the Madagascar fragment from the southwest of the Indian subcontinent, possibly triggered by the Marion hotspot volcanism. A portion of this chapter has been published in “Geophysical Journal International” (Sreejith et al., 2008. *Geophys. J. Int.*, 175, 729-741).

**Chapter 5** address two important geophysical aspects of the 85°E Ridge i) isostasy, ii) the contrasting gravity anomalies of the ridge: negative anomaly for the northern part (north of 5°N) and positive for the southern part. The morphology, extent, trend and characteristic gravity signatures are studied in detail using seismic reflection, satellite and ship-borne gravity data of the northeastern Indian Ocean. Multichannel seismic reflection and gravity data along four profiles crossing the 85°E Ridge at 14.7°, 14°, 13° and 4.5°N latitudes are modeled using process oriented method in order to determine the structure, isostasy and long-term mechanical properties of the lithosphere beneath the ridge. The results suggest that the 85°E Ridge was emplaced on approximately 10-15 km thick elastic plate ( $T_e$ ) and in off-ridge tectonic setting. The change of gravity anomalies through time from its inception (positive anomaly) to present (negative anomaly) is demonstrated by computation of gravity anomalies for different mantle-crust-sediment structural models of the ridge existent at three geological ages, late Cretaceous, early Miocene and Recent. The present results and published plate reconstruction information together opines that the 85°E Ridge was emplaced by a short-lived hotspot from 85 to 55 Ma in an intraplate geological setting. Recently, a portion of this chapter has been accepted for publication in “Journal of Earth System Science”.

**Chapter 6** deals with the isostatic compensation mechanism and crustal structure of the Ninetyeast Ridge. Seventy two bathymetry and gravity profiles (ship-born and satellite derived) running across the Ninetyeast Ridge, spread between 28°S and 8°N latitudes with an interval of approximately 50 km, are utilized for the admittance analysis and flexural modeling in order to determine the elastic plate thickness ( $T_e$ ) beneath the ridge. The southern (south of 22°S latitude) and northern (north of 2°N latitude) parts of the ridge are flexurally compensated with elastic plate thickness ( $T_e$ ) values of >10 and >18 km, respectively. Admittance analysis suggests that the central part of the ridge (between latitudes 20°S and 2°N) has Airy type compensation with crustal thickness 15-20 km.

However,  $T_e$  values derived along profiles using flexural modeling, revealed that that central part of the ridge could be further divided into 1) south-central part ( $18^\circ\text{S}$  to  $8^\circ\text{S}$ ), where the  $T_e$  values constantly decrease from 20 to 5 km and 2) north-central part ( $8^\circ\text{S}$  to  $2^\circ\text{N}$ ), where  $T_e$  values randomly vary between 2 and 25 km. Further, the ridge crustal structure was derived along five representative profiles (with different  $T_e$  values) by using gravity forward modeling under the constraints of seismic reflection and refraction results. Based on the present results and published plate reconstruction results, a convincing evolutionary model is proposed for the evolution of the underneath oceanic lithosphere and emplacement of the Ninetyeast Ridge. The southern part of the ridge was emplaced on a lithosphere of intermediate strength possibly along the edge of the Indian plate, whereas northern part of the ridge was emplaced in an intraplate setting. The highly variable isostatic compensation mechanism in the central part of the ridge could be a manifestation of complex interactions between the Kerguelen hotspot and spreading ridge segments. The north-central part of the ridge may have emplaced on a crust of highly variable age produced by multiple southward ridge jumps, whereas the south-central part was emplaced on a crust of uniformly increasing age towards south produced as a result of a major southward ridge jump.

**Chapter 7** summarizes and synthesizes important results with future outlook.

# CONTENTS

|  |             |
|--|-------------|
| Statement  | i           |
| Certificate  | ii          |
| Acknowledgments  | iii         |
| Preface  | v           |
| List of Tables   | xiii        |
| List of Figures  | xiv         |
| <br>   |             |
| <b>CHAPTER 1 Introduction</b>  | <b>1-25</b> |
| <br>   |             |
| 1.1 General  | 2           |
| 1.2 Plate Tectonics  | 3           |
| 1.2.1 Plate Boundaries   | 6           |
| 1.2.2 Continental Margins and Ocean Basins                           | 9           |
| 1.2.3 Fracture Zones   | 10          |
| 1.2.4 Age of the Ocean Floor   | 10          |
| 1.3 Mantle Plumes and Hotspots                                       | 11          |
| 1.3.1 Three Distinct Types of Hotspots                               | 12          |
| 1.3.2 Hotspot Expressions on Lithospheric Plates                     | 15          |
| 1.3.3 Fixity of Hotspots   | 16          |
| 1.4 Aseismic Ridges  | 16          |
| 1.4.1 Aseismic Ridges- Record of Absolute and Relative Plate Motions | 17          |
| 1.5 Concept of Isostasy  | 18          |
| 1.5.1 Isostatic Compensation Mechanisms                              | 19          |
| 1.5.1.1 Airy–Heiskanen Model   | 20          |
| 1.5.1.2 Pratt–Hayford Model  | 21          |
| 1.5.1.3 Vening Meinesz Model   | 22          |
| 1.6 Elastic Plate Thickness and Flexural Rigidity                    | 23          |
| 1.7 Isostatic Compensation of Aseismic Ridges and Seamounts          | 23          |
| 1.8 Objectives   | 24          |

|   |              |
|---|--------------|
| <b>CHAPTER 2 Aseismic Ridges of the Northeastern Indian Ocean</b>                       | <b>26-37</b> |
| 2.1 Evolution of the Indian Ocean   | 27           |
| 2.2 Major Aseismic Ridges   | 32           |
| 2.2.1 The Ninetyeast Ridge  | 32           |
| 2.2.2 The Chagos-Laccadive Ridge  | 32           |
| 2.2.3 The 85°E Ridge  | 34           |
| 2.2.4 The Comorin Ridge   | 35           |
| 2.2.5 The Broken Ridge  | 35           |
| 2.3 Other Major Structural Features   | 35           |
| 2.3.1 The Kerguelen Plateau   | 36           |
| 2.3.2 The Elan Bank   | 36           |
| 2.3.3 The Afanasy Nikitin seamount  | 37           |
| <br>  |              |
| <b>CHAPTER 3 Methodology and Geophysical Data</b>                                       | <b>38-53</b> |
| 3.1 Introduction  | 39           |
| 3.2 Gravity Measurements at Sea   | 40           |
| 3.3 Gravity Anomaly Computation   | 40           |
| 3.3.1 The Latitude Correction   | 41           |
| 3.3.2 The Free-air Correction and Free-air Gravity Anomaly                              | 41           |
| 3.3.3 The Eötvös correction   | 42           |
| 3.4 Interpretation of Gravity Anomaly using Two-dimensional Gravity<br>Forward Modeling | 42           |
| 3.5 Theoretical Basis of Isostatic Compensation   | 44           |
| 3.5.1 Isostatic Response Functions  | 45           |
| 3.5.2 The Gravitational Admittance  | 46           |
| 3.5.3 Gravitational Admittance and Isostatic Models                                     | 47           |
| 3.6 Computation of Admittance from Observed Data  | 50           |
| 3.7 Process Oriented Gravity Modeling   | 51           |
| 3.8 Geophysical Data  | 53           |

|   |               |
|---|---------------|
| <b>CHAPTER 4 Structure and Isostasy of the Comorin Ridge</b>  | <b>54-82</b>  |
| 4.1 Introduction  | 55            |
| 4.2 Geological Setting of the Region  | 57            |
| 4.3 Geophysical Data  | 58            |
| 4.4 Bathymetry, Gravity and Magnetic Anomalies of the Comorin Ridge   | 58            |
| 4.5 Gravity-Topography Admittance Analysis  | 62            |
| 4.5.1 Elastic Plate Thickness and Crustal Thickness   | 62            |
| 4.5.2 $T_e$ and Age of Emplacement of the Comorin Ridge   | 68            |
| 4.6 Crustal Structure of the Comorin Ridge- Two-Dimensional Gravity Forward Modeling  | 70            |
| 4.6.1 Crustal Structure of the Southern Comorin Ridge   | 70            |
| 4.6.2 Crustal Structure of the Northern Comorin Ridge   | 71            |
| 4.7 Continent-Ocean Boundary on Western Margin of Sri Lanka and Southern Tip of India   | 75            |
| 4.8 Tectonics and Evolution of the Comorin Ridge  | 78            |
| <br>  |               |
| <b>CHAPTER 5 The 85°E Ridge – Study of Crustal Structure, Isostasy and Negative Gravity Anomaly using Process Oriented Gravity Modeling</b> | <b>83-114</b> |
| 5.1 Introduction  | 84            |
| 5.2 Tectonic Setting  | 87            |
| 5.3 Geophysical Data  | 87            |
| 5.4 Seismic Structure and Gravity Anomaly of the 85°E Ridge   | 88            |
| 5.5 Magnetic Response of the 85°E Ridge   | 95            |
| 5.6 Process Oriented Gravity Anomaly Modeling   | 95            |
| 5.7 Elastic Plate Thickness and Crustal Structure of the 85°E Ridge   | 96            |
| 5.7.1 Crustal Structure of 85°E Ridge- Two-Dimensional Gravity Forward Modeling   | 100           |
| 5.8 Different Stages of the 85°E Ridge - Simulation of Gravity Anomalies  | 109           |
| 5.9 Structure and Tectonics of the 85°E Ridge   | 111           |

|  |                |
|--|----------------|
| <b>CHAPTER 6 Spatial Variations in Isostatic Compensation Mechanisms of the Ninetyeast Ridge and their Tectonic Implications</b> | <b>115-153</b> |
| 6.1 Introduction   | 116            |
| 6.2 Geophysical Data   | 120            |
| 6.2.1 Sediment Corrections   | 123            |
| 6.2.2 Slab Residual Gravity Anomaly Computation  | 123            |
| 6.3 Bathymetry and Gravity Anomalies of the Ninetyeast Ridge   | 124            |
| 6.4 Elastic Plate Thickness along the Ninetyeast Ridge   | 126            |
| 6.4.1 Flexural Modeling  | 127            |
| 6.4.2 Admittance Analysis  | 133            |
| 6.5 Crustal Structure of the Ninetyeast Ridge  | 139            |
| 6.6 Variations of $T_e$ values along the Ninetyeast Ridge and Geodynamic Implications  | 146            |
| <br>   |                |
| <b>CHAPTER 7 Summary and Conclusions</b>   | <b>154-164</b> |
| 7.1 The Structure and Isostatic Model of the Comorin Ridge   | 155            |
| 7.2 The Structure and Evolution of the 85°E Ridge  | 157            |
| 7.3 The Structure and Tectonics of the Ninetyeast Ridge  | 159            |
| 7.4 Future Research  | 161            |
| 7.4.1 Continent-Ocean Boundary on Western Margin of Sri Lanka and Southern Tip of India  | 162            |
| 7.4.2 Origin of the 85°E Ridge   | 162            |
| 7.4.3 Variable Isostatic Compensation Mechanism beneath the Ninetyeast Ridge and its Complex Tectonic Evolution                  | 163            |
| <br>   |                |
| <b>References</b>  | <b>165</b>     |
| <br>   |                |
| <b>List of Publications from the Present Research Work</b>   | <b>182</b>     |

## **List of Tables**

|     |   |     |
|-----|---|-----|
| 4.1 | Model parameters used for the calculation of theoretical admittance                                 | 63  |
| 4.2 | Elastic plate thickness ( $T_e$ ) and crustal thickness ( $t$ ) determined from admittance analysis | 65  |
| 5.1 | Model parameters used for the flexural calculations and gravity modeling                            | 98  |
| 6.1 | Model parameters used for the flexural computations   | 128 |
| 6.2 | Best fit $T_e$ values along Ninetyeast Ridge (south to north) obtained by flexural modeling         | 129 |
| 6.3 | Mean density and water depth derived from the slope and intercept of admittance                     | 136 |

## List of Figures

| <b>Figure</b>  | <b>No.</b> |
|--|------------|
| 1.1 Disposition of major tectonic plates on the Earth  | 4          |
| 1.2 Schematic sketch of vertical cross-section through lithospheric plates illustrating different plate boundaries                     | 7          |
| 1.3 A schematic cross section of the dynamic earth along its rotational axis   | 13         |
| 1.4 Global distribution of three types of hotspots   | 14         |
| 1.5 Isostatic compensation according to Airy- Heiskanen model  | 20         |
| 1.6 Isostatic compensation according to Pratt–Hayford model  | 21         |
| 1.7 Isostatic compensation according to Vening Meinesz elastic plate model   | 22         |
| 2.1 Reconstruction of Gondwana super-continent from Jurassic to Present  | 28         |
| 2.2. General bathymetric map of Indian Ocean   | 33         |
| 3.1 Polygon approximation of irregular vertical section of two-dimensional body  | 43         |
| 3.2 Elastic plate approximation of the bending oceanic lithosphere under load  | 45         |
| 3.3 Elastic plate model for layered oceanic crust  | 49         |
| 3.4 The principle of backstripping   | 52         |
| 4.1 General bathymetry of the southern tip of India and south and west margins of Sri Lanka  | 56         |
| 4.2 Three dimensional view of the Comorin Ridge surface topography   | 59         |
| 4.3 Composite plots of bathymetry, gravity and magnetic profile data across the Comorin Ridge and its vicinity                         | 60         |
| 4.4 Admittance values computed for individual profiles plotted with theoretical curves for <b>a)</b> Airy and <b>b)</b> Flexure models | 64         |
| 4.5 Aadmittance, coherence and phase in degree generated from <b>a)</b> southern <b>b)</b> northern set profiles                       | 66         |



|               |   |     |
|---------------|---|-----|
| <b>4.6</b>    | The gravity energy generated from <b>a)</b> southern <b>b)</b> northern profiles  | 67  |
| <b>4.7</b>    | Observed admittance with standard error bars generated from <b>a)</b> southern <b>b)</b> northern profiles with theoretical models        | 69  |
| <b>4.8</b>    | Two-dimensional gravity model with interpreted crustal structure along profile C1215  | 72  |
| <b>4.9</b>    | Two-dimensional gravity model with interpreted crustal structure along profile V3307 considering that the underneath crust is continental | 73  |
| <b>4.10</b>   | Two-dimensional gravity model with interpreted crustal structure along Profile V3307 considering that the underneath crust is Oceanic     | 74  |
| <b>4.11</b>   | A comparison of bathymetry, gravity and magnetic profile data from WCMI, ECMI and western margin of Sri Lanka                             | 77  |
| <b>4.12</b>   | Interpreted COB on western margin of Sri Lanka and southern tip of India  | 79  |
| <b>4.13</b>   | Late Cretaceous reconstruction of India, Madagascar, Seychelles and Africa with reference to the Marion hot spot position                 | 81  |
| <b>5.1</b>    | Ship-borne gravity profiles of the NE Indian Ocean. Free-air gravity anomalies plotted at right angle to the ship tracks                  | 85  |
| <b>5.2</b>    | Satellite derived free-air gravity anomaly map of the NE Indian Ocean   | 89  |
| <b>5.3 a)</b> | Seismic sections of 85°E Ridge in Mahanadi Offshore Basin   | 91  |
| <b>b)</b>     | Seismic sections of the 85°E Ridge from 8°N to ANS  | 92  |
| <b>c)</b>     | MAN-01 and SK107-07 seismic reflection sections and its interpreted line diagrams across 85°E Ridge stacked with gravity anomaly          | 93  |
| <b>d)</b>     | MAN-03 and 98791 seismic reflection sections and its interpreted line diagrams across 85°E Ridge stacked with gravity anomaly             | 94  |
| <b>5.4</b>    | Simplified flow diagram of process oriented modeling  | 97  |
| <b>5.5</b>    | The ridge and sedimentation anomalies computed for different $T_e$ values through process oriented gravity modeling                       | 99  |
| <b>5.6</b>    | Velocity-depth relation for Bay of Bengal sediments   | 101 |

|   |     |
|---|-----|
| <b>5.7 a)</b> Crustal structure of 85°E Ridge along profile MAN-01 along with different anomaly components  | 102 |
| <b>b)</b> Crustal structure of 85°E Ridge along profile SK107-07 along with different anomaly components  | 103 |
| <b>c)</b> Crustal structure of 85°E Ridge along profile MAN-03 along with different anomaly components  | 104 |
| <b>d)</b> Crustal structure of 85°E Ridge along profile 98791 along with different anomaly components   | 105 |
| <b>5.8 a)</b> Two-dimensional gravity modeling and interpreted crustal structure along profile MAN-03   | 107 |
| <b>b)</b> Two-dimensional gravity modeling and interpreted crustal structure along profile-98791  | 108 |
| <b>5.9</b> Reconstruction of the gravity anomalies over the 85°E Ridge through geological ages for profiles <b>a)</b> MAN-01, <b>b)</b> SK 107-07, <b>c)</b> MAN-03 | 110 |
| <b>5.10</b> Late cretaceous and Paleocene reconstruction of northeastern Indian Ocean   | 114 |
| <b>6.1</b> Satellite derived bathymetry map of the northeastern Indian Ocean  | 117 |
| <b>6.2</b> Satellite derived free-air gravity anomaly map of the NE Indian Ocean  | 119 |
| <b>6.3 a)</b> Comparison of gravity data along profile A2093111 with satellite data   | 121 |
| <b>b)</b> Comparison of bathymetry data along profile A2093111 with satellite derived and ETOPO-1 bathymetry data   | 121 |
| <b>c)</b> Comparison of bathymetry data along profile A2093111 with satellite derived and ETOPO-1 bathymetry data in spectral domain                                | 122 |
| <b>6.4 a)</b> Observed bathymetry and gravity anomaly of Profile S52 along with sediment corrections  | 125 |
| <b>b)</b> Computation of the gravity effect of the subducting Indian Ocean lithosphere  | 125 |
| <b>6.5</b> Variations of $T_e$ values derived from flexural modeling along Ninetyeast from 28°S to 8°N  | 130 |
| <b>6.6 a)</b> Flexural modeling along selected profiles from south and south-central part of the Ninetyeast Ridge   | 131 |

|               |   |     |
|---------------|---|-----|
| <b>b)</b>     | Flexural modeling along selected profiles from north-central and northern part of the Ninetyeast Ridge  | 132 |
| <b>6.7 a)</b> | Observed admittance, coherence, phase and gravitational energy plots for southern part of the Ninetyeast Ridge                                      | 134 |
| <b>b)</b>     | Observed admittance, coherence, phase and gravitational energy plots for south-central part of the Ninetyeast Ridge                                 | 134 |
| <b>c)</b>     | Observed admittance, coherence, phase and gravitational energy plots for north-central part of the Ninetyeast Ridge                                 | 135 |
| <b>d)</b>     | Observed admittance, coherence, phase and gravitational energy plots for northern part of the Ninetyeast Ridge                                      | 135 |
| <b>6.8 a)</b> | Observed admittance with standard error bars generated from profiles in the southern part of the Ninetyeast Ridge with Airy and Flexure models      | 137 |
| <b>b)</b>     | Observed admittance with standard error bars generated from profiles in the south-central part of the Ninetyeast Ridge with Airy and Flexure models | 137 |
| <b>c)</b>     | Observed admittance with standard error bars generated from profiles in the north-central part of the Ninetyeast Ridge with Airy and Flexure models | 138 |
| <b>d)</b>     | Observed admittance with standard error bars generated from profiles in the northern part of the Ninetyeast Ridge with Airy and Flexure models      | 138 |
| <b>6.9</b>    | Two-dimensional gravity model with interpreted crustal structure along profile V1811  | 141 |
| <b>6.10</b>   | Two-dimensional gravity models with interpreted crustal structure along profile V3305   | 142 |
| <b>6.11</b>   | Two-dimensional gravity models with interpreted crustal structure along profile SK28-3  | 143 |
| <b>6.12</b>   | Two-dimensional gravity models with interpreted crustal structure along profile SK28-34   | 144 |
| <b>6.13</b>   | Two-dimensional gravity models with interpreted crustal structure along profile S52   | 145 |
| <b>6.14</b>   | Age verses latitude plots for Ninetyeast Ridge  | 151 |
| <b>6.15</b>   | Comparison of the proposed evolutionary model of Ninetyeast Ridge with the existing models  | 153 |

## Introduction

- 1.1 General
- 1.2 Plate Tectonics
  - 1.2.1 Plate Boundaries
  - 1.2.2 Continental Margins and Ocean Basins
  - 1.2.3 Fracture Zones
  - 1.2.4 Age of the Ocean Floor
- 1.3 Mantle Plumes and Hotspots
  - 1.3.1 Three Distinct Types of Hotspots
  - 1.3.2 Hotspot Expressions on Lithospheric Plates
  - 1.3.3 Fixity of Hotspots
- 1.4 Aseismic Ridges
  - 1.4.1 Aseismic Ridges- Record of Absolute and Relative Plate Motions
- 1.5 Concept of Isostasy
  - 1.5.1 Isostatic Compensation Mechanisms
    - 1.5.1.1 Airy–Heiskanen Model
    - 1.5.1.2 Pratt–Hayford Model
    - 1.5.1.3 Vening Meinesz Model
- 1.6 Elastic Plate Thickness and Flexural Rigidity
- 1.7 Isostatic Compensation of Aseismic Ridges and Seamounts
- 1.8 Objectives

## Introduction

### 1.1 General

The Indian Ocean is youngest in age and smallest in area relative to the other major oceans, Atlantic and Pacific Oceans. But its structure and evolution are very complex and the ocean encompasses with almost all varieties of geological processes. A systematic scientific study of the Indian Ocean has started after successful completion of the International Indian Ocean Expedition (IIOE) during the period 1960-65. Geological and geophysical data of the IIOE and subsequent major scientific expeditions including the Deep Sea Drilling Project (DSDP) and the Ocean Drilling Program (ODP) have brought out broader understanding of geodynamic evolution of the Indian Ocean since the break-up of eastern Gondwanaland in early Cretaceous. However, major scientific aspects like precise timing of continental break-up, continental margin evolution, hotspot activity, formation of aseismic ridges etc. are not fully understood.

The structural framework of the northeastern Indian Ocean is unique as the region includes numerous oceanic fracture zones, aseismic ridges, seamounts, abandoned spreading centers, Sunda subduction zone, etc. Besides, the ocean floor is carpeted by enormously thick pre- and post- continental collision sediments discharged from the rivers of east coast of India, Ganges and Brahmaputra. Three aseismic ridges, 85°E Ridge, Ninetyeast Ridge and Comorin Ridge are the major structural features in the northeastern Indian Ocean. The Ninetyeast Ridge is a product of the Kerguelen hotspot activity, whereas varied opinions exist for the origin of the 85°E Ridge. The Comorin Ridge is one of the least studied aseismic ridges and a little is known regarding its origin and isostasy. Crustal structure, isostasy and origin of these aseismic ridges are key elements to better understand the tectonic evolution of the Indian Ocean lithosphere.

## 1.2 Plate Tectonics

The theory of *Plate Tectonics* in earth science is a relatively new scientific postulation and it has revolutionized our understanding of the dynamic planet Earth, upon which we live. In geology the word “plate” refers to thin and rigid slab of rocks, whereas “tectonics” term comes from the Greek root “to build”. Plate tectonic theory suggests that outer most layer of the Earth is fragmented into numerous segments of varying size and the segments are being moved relative to each other over a fluid substratum (asthenosphere). These segments are called lithospheric or tectonic plates. The average thickness of the lithospheric plate is 100 km and consists of crust and upper part of mantle. The fluid layer below the lithosphere up to a depth of ~ 670 km is referred as asthenosphere. The asthenosphere is being heated by radioactive elements such as Uranium, Thorium, and Potassium and the rocks are partially molted and led to convection currents, which eventually drive the rigid lithospheric plate over the asthenosphere with relatively little resistance. The disposition of major tectonic plates of the Earth is illustrated in Figure 1.1.

The idea of moving continents was existing much before the advent of plate tectonic theory. In 1912 Alfred Lothar Wegener postulated that continents were once compressed into a single protocontinent, which he called Pangaea (meaning "all lands"), and over the time they have drifted apart and reached to the current distribution. Wegener's continental drift hypothesis (Wegener, 1922) was mainly based on the observation that most of the continents appears to fit together like a puzzle such as the West African coastline seems to snuggle nicely into the east coast of South America. A more close fit is observed if submerged continental shelf is considered rather than the present-day coastline. The other evidences supporting the hypothesis includes 1) occurrence of same fossilized plants and animals from the same time period across continents 2) similarity in rock formations 3) striae left by the scraping of glaciers over the land surfaces. Further, Wegener's drift hypothesis has provided an explanation for mountain building process; the leading edge of the drifting continents would encounter resistance and thus compress and fold upwards for forming mountains. Wegener also suggested that India drifted northward into the Asia forming the Himalayas.

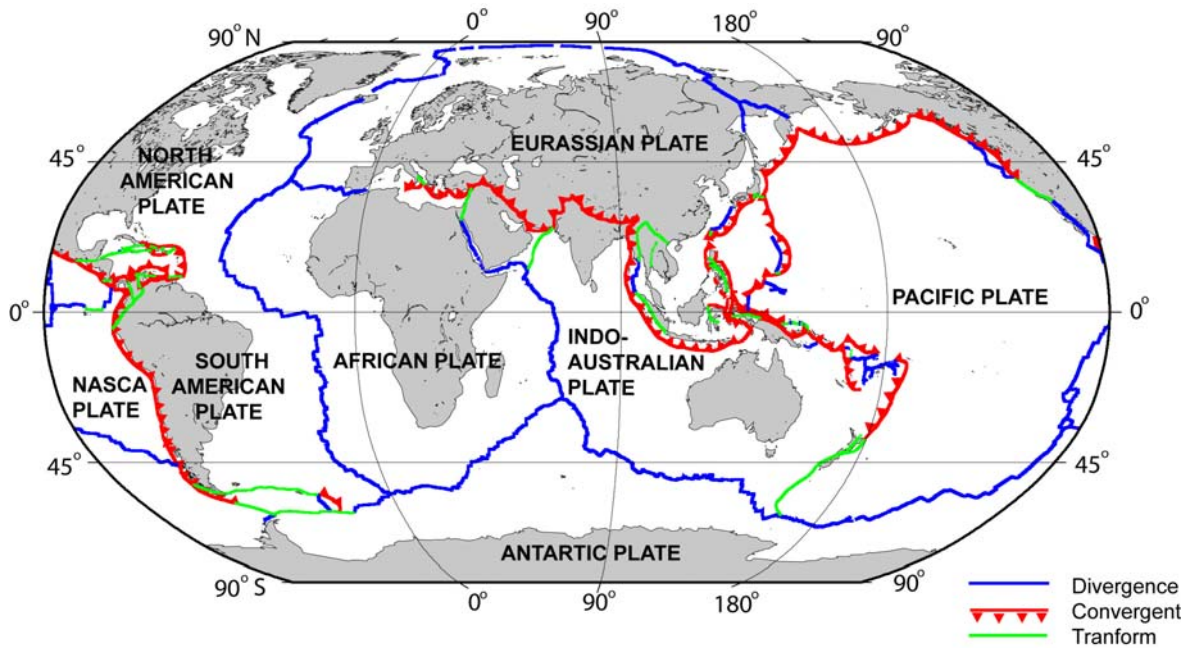


**Figure 1.1** Disposition of major tectonic plates on the Earth. Divergent, convergent and transform plate boundaries are also shown.

Though the theory of continental drift would become the spark that ignited a new way of viewing the Earth, it terribly failed to explain the nature of forces, which propelled giant and massive continents around the surface of the Earth. Wegener's model of continental movement over ocean floor, like boat on the surface of water, was rejected by the scientific community and then theory remained dormant until the discovery of *Seafloor Spreading* theory (Hess 1960, 1962; Dietz, 1961). This theory suggests that new magma from deep within the Earth rises easily through the weak zones and eventually erupts along the ridge crest to create a new oceanic crust. Further, the new oceanic crust generated at the ridge crest moves away like a conveyer belt motion, and finally descends down to mantle along deep-trenches, hence the total surface area of the Earth essentially remains constant. The most definitive evidence for seafloor spreading process comes from study of the linear magnetic anomalies that characterizes the ocean floor. The Earth's magnetic field in the geological past has flip-flopped several times, when the magma cools down through Curie temperature it acquires the Earth's prevailing magnetic polarity leading to zebra-like magnetic strips of normal and reverse polarity parallel to the ridge system. This hypothesis was supported by several lines of evidence: (1) at or near the crest of the ridge, the rocks are very young, and they become progressively older away from the ridge crest; (2) the youngest rocks at the ridge crest always have present-day (normal) polarity; and (3) stripes of rock parallel to the ridge crest alternated in magnetic polarity recording the history of the Earth's magnetic field reversals. Vine and Mathews (1963) and independently by Morley and Larochelle explained the seafloor spreading theory in the light of Earth's magnetic reversals, and later the theory was known as Vine and Mathews seafloor spreading hypothesis.

Thus, the continental drift hypothesis with strong support from seafloor spreading hypothesis framed the basic concepts of tectonic plates and their internal dynamics. The actual mechanism of plate motion was explained by the mantle convection phenomena by Tuzo Wilson (1965, 1966). Below the lithospheric plates, at some depth the mantle is partially molten and can flow, albeit slowly, in response to steady forces applied for long periods of time. Hot magma rises below the mid-oceanic ridge system, spreads latterly



carrying the plates and finally cold plates decent down to mantle, where the plate material is reheated and leading to another cycle. Though mantle convection and seafloor spreading provided a basic mechanism of plate tectonics, recent studies show that “slab pull” created by the sinking lithospheric plates at subduction zones are more prominent driving forces.

### **1.2.1 Plate Boundaries**

Plate boundaries are geodynamically active deformed zones, where a large fraction of earthquakes, volcanic eruptions and mountain building take place. Plate boundaries are broadly classified as divergent, convergent, transform and diffuse (Figures 1.1 and 1.2).

Along the divergent boundaries lie along the spreading centers, lithospheric plates are created by the up-welling of magma from the mantle. The two plates from either side of the ridge crest move away in opposite direction with almost equal velocities of few centimeters per year. The gap generated by the diverging plate is filled by the hot, molten rocks from the mantle. The up-welled mantle rocks subsequently cool down due to conductive heat rocks and accrete to the base of the spreading plates. As the plates move away from the spreading centre, they cool down, become denser and thicker leading to subsidence. The divergent boundary or the ridge crest is topographically elevated due to greater buoyancy of the thinner and hotter lithosphere. A component of the gravitational body force of the elevated lithosphere drives the plates away from the accretionary boundary. This gravitational sliding forms an important force called “ridge push” which eventually drives the plates. The lithospheric plates created at the divergent plate boundaries are being destroyed almost at the same rate to keep the total surface area of the Earth constant. Away from the ridge crest, the old, dense and thick lithosphere becomes gravitationally unstable and sinks into the mantle along oceanic trenches or convergent plate boundaries. The descending plate creates negative buoyancy forces which get transmitted to the surface of the entire plate casing pulling towards the trench. This is the most important force that drives the plates and hence causes continents to move and known as “slab pull”. The immense stress involved in the subduction dynamics results numerous high-magnitude earthquakes along the subduction zones. The locations of these deep

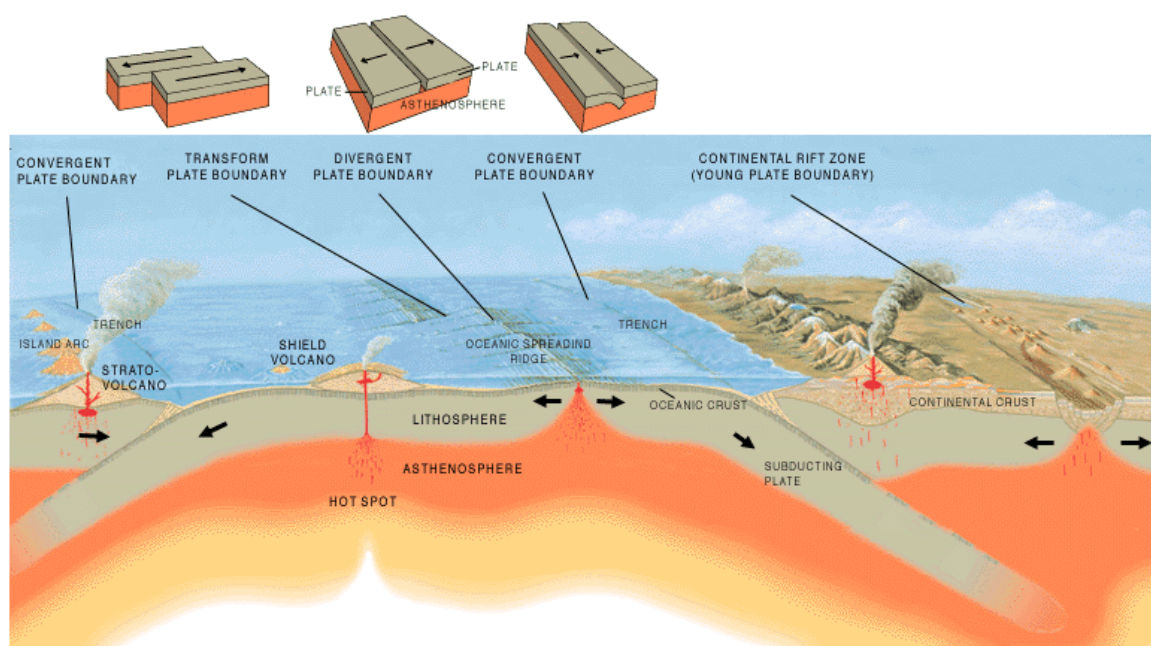


**Figure 1.2** Schematic sketch of vertical cross-section through lithospheric plates illustrating different plate boundaries (after Kious and Tilling, 2008)

earthquakes define the structure of descending plate and are known as Wadati-Benioff Zone.

Convergence can occur between oceanic and continental plates, between two oceanic plates and between two continental plates. An oceanic-continent convergence leads to the subduction of denser oceanic plate under the lighter continental plate, for example, off west coast of South America the Nazca plate is being subducted under continental part of the South American plate along the Peru-Chile trench. When two oceanic plates converge, the older and denser plate subducts beneath the other. Subduction processes in oceanic-oceanic plate convergence also result in the formation of chain of volcanoes and island arcs. The Mariana Islands were created due to the excessive volcanism when fast moving Pacific plate converges against the slower moving Philippine plate along the Mariana trench. When two continents converge, they resist downward motion and tend to buckle and push upwards as continental rocks are relatively lighter. The slow continuous convergence of the Indian and Eurasian plates over millions of years resulted the formation of the Himalayan ranges.

The zone between two divergent plates or between the spreading centers, where sliding takes place horizontally is called transform-fault boundary. Most of the transform faults are found on ocean floor offsetting mid-oceanic ridge into numerous segments. The ridge segments lie perpendicular to the spreading direction, whereas transform faults lie parallel to the spreading direction. The relative velocity across the fault segments causes earthquakes, which are more intense than the spreading related seismicity. The transform fault can also connect two trench segments or can terminate at a triple junction of three lithospheric plates.

Diffuse plate boundaries are broad zones, in which boundaries are not very well defined and the effects of plate interaction are unclear. Diffuse plate boundary mapped in the central Indian Ocean is the best example of such plate boundary zones. It has divided the traditionally believed Indo-Australian plate into three component plate; India, Australia and Capricorn (Royer and Gordon et al., 1997; Gordon et al., 1998)

### 1.2.2 Continental Margins and Ocean Basins

Ocean basins and continental platforms are most dominant physiographic domains on the surface of the Earth (Kenneth, 1982). These are linked by continental margins, where the oceanic and continental crust merges along a narrow transition zone. Continental margins form about 20% of the total area of oceans. Morphologically continental margin is divided into continental shelf, slope and rise. Continental shelf consists of gently sloping flat laying area and extends from shoreline to shelf edge. The shelf is a seaward extension of continent and covered by the sediments derived from the land. At the edge of the continental shelf, the water depth abruptly increases from 100-200 m to 1500-3500 m within a short horizontal distance and form a continental slope. The low relief-gently dipping province between the continental slope and ocean basin is called continental rise. The continental margins are best store houses of sediment accumulations transported from the continents.

Continental margins are broadly classified into two types, Passive or Atlantic and Active or Pacific. Passive continental margins develop when continents break and rift apart and allow forming the ocean floor between the rifted continental blocks. Initially the passive margins form at divergent plate boundaries and with time they move apart due to the commencement of seafloor spreading and also subside with cooling. Eventually they become sites of massive sedimentation and subsidence. A well-developed shelf-slope-system is observed in most of the passive continental margins. Active continental margins are formed at convergent plate boundaries. They are associated with a narrow shelf and a deep trench or island arch system and are regions of intense seismic activity.

Ocean basins lie between continental margins and to the vicinity of mid-oceanic ridges, include abyssal planes, oceanic rises and seamounts and seamount chains. Abyssal plains, in general, lie in the regions of flattest portions of Earth's surface with a slope less than a meter per km horizontal distance. The topographic undulations of the ocean floor are covered with sediments mainly derived from the continents. They extend from 200 km to 2000 km long with a depth ranging from 3000 m to 6000 m. Abyssal hills are small,

sharply defined topographic rises of elevation less than 1000 m and with a few tens of kilometers horizontal extents. They occur in groups between abyssal plains and mid-oceanic ridges. Abyssal hills are integral part of the mid-oceanic ridge system, but are morphologically distinct with smaller dimensions, deeper occurrence and often buried under sediments. Volcanic edifices in the ocean basin that rise above 1000 m from the adjacent ocean floor are called seamounts. They occur either in cluster or distributed randomly in the ocean basins. Seamounts rise abruptly from the ocean floor with deeply buried base and usually have steep slopes with conical shape. Seamounts, which were formed above sea surface, becomes flat topped due to erosion and sinks at later period to form Guyots or table mountains. Guyots are commonly found in the Pacific Ocean.

### **1.2.3 Fracture Zones**

Fracture zones are long, arcuate and narrow geological features on ocean floor. A typical fracture zone is of about 60 km wide with several hills and valleys aligned along the overall trend (Cox and Hart, 1986). Fracture zones cut across major features of ocean floor including rises, abyssal plains and mid-oceanic ridges. They resemble strike-slip faults in topography and large off-sets when cut across magnetic isochrones and mid-ocean ridges. Unlike active faults, fracture zones are mostly devoid of seismic activity all along their length. However, portion of the fracture zone, which offset the ridge axis is seismically very active and this portion is called transform fault. This is due to the intense shearing between the ridge segments along the transform fault. In other words, transform fault becomes a part of a plate boundary and allows the plates to move in opposite directions. Identification of fracture zones on ocean floor is extremely important as they provide explicit clues to reveal the tectonic history of the continents and oceans.

### **1.2.4 Age of the Ocean Floor**

Plate tectonic theory explains the strips of positive and negative marine magnetic anomalies as the thermal remnant magnetism of oceanic crust produced during episodic reversals of the Earth's magnetic fields. The strips of seafloor with positive magnetic anomalies were created during periods of normal polarity of the Earth's magnetic field and

those with negative magnetic anomalies were produced during periods of reversed polarity of the Earth's magnetic field. The magnetic anomaly pattern is used to date the ocean floor by correlating with the ages of magnetic field reversals obtained by paleomagnetic and isotopic dating results. The distribution of ocean floor ages determined by magnetic anomaly identifications, have been subsequently validated using dates of basaltic rocks and deep sediment cores obtained from Deep Sea Drilling Project. Isochrone or portion of ocean crust formed at same age is parallel and symmetrical to the mid-oceanic ridge. However, they are at places offset by hundreds of kilometers by fracture zones.

### **1.3 Mantle Plumes and Hotspots**

Mantle plumes are quasi-cylindrical concentrated upwelling of hot mantle rock and they represent a basic form of mantle convection, whereas hotspots are anomalous areas of surface volcanism that cannot be linked with plate tectonic processes (Morgan, 1971, 1972). Hotspots are caused by upwelling of mantle rocks from a deep thermal boundary layer below the upper mantle; they are driven by thermal buoyancy rather responding to plate tectonics and subduction. The classical hotspot model proposed by Wilson (1963) and Morgan (1971, 1972) requires magma source deep in the mantle and thus the rising magma are chemically distinct from those of mid-oceanic ridges. Further, their nearly stationary mantle plumes on the base of moving lithospheric plate could explain the age progression of volcanic chains.

Numerical simulation and laboratory experiments show that the plumes initiate with a leading plume head followed by a narrow conduit or plume tail connecting the plume head to the source region (Turcotte and Schubert, 2002). Supporting this result, observational evidences suggest that flood basalt eruptions mark the initiation of hotspots. For example, the Reunion hotspot track originates from Deccan flood basalt province of western India (White and McKenzie, 1989).

However, recent studies shows that very few hotspots are associated with upper or lower mantle tomographic anomalies, but majority lack prominent swells or surface volcanism

(Anderson, 2007; and references therein). Among the prominent swell hotspots many are lacking geochemical evidences for its deeper origin. Most significant and geochemically distinct hotspots like Hawaii, Iceland and Reunion are not underlined by lower mantle P-wave seismic anomalies. These studies have lead to an alternate hypothesis that the anomalous volcanism is attributed to plate tectonic processes at the Earth's top thermal boundary layer. Below the tectonic plates the mantle is at near melting point temperature, and it is inhomogeneous by the recycling of crustal rocks, these two conditions can cause volcanism and this is controlled by the stress conditions of the plate. The most significant processes that cause stress to vary in the lithosphere are differential cooling and variable plate boundary types. Thus according to this model, anomalous volcanism occurs, where the stress field is extensional and mantle is unusually fusible, therefore this model does not requires temperature anomalies deep in the mantle. A comparison of these two contrasting models of hotspot formation is given in Figure 1.3.

### **1.3.1 Three Distinct Types of Hotspots**

Courtillot et al. (2003) made an attempt to classify 49 hotspots on the Earth based on geochemical, geochronological, geophysical results (Figure 1.4). The characteristic features of deep origin hotspots are presence of linear volcanic chain, flood basalts at the origin, prominent buoyancy, high He isotopic ratios and low shear wave velocities at the mantle. Only seven out of 49 hotspots meet at least three of the above criteria and classified as primary hotspots. Around twenty hotspots are classified as secondary-type hotspots as they originate at shallow depths from the transient stems of super plumes. The remaining hotspots must have originated by stress related cracking of lithosphere as suggested by Anderson (2007). It is interesting to note that the three different hotspots are, in general, associated with three different thermal boundaries within the Earth. Hence, these hotspots should be studied independently keeping their different mechanisms of formation to avoid controversies.

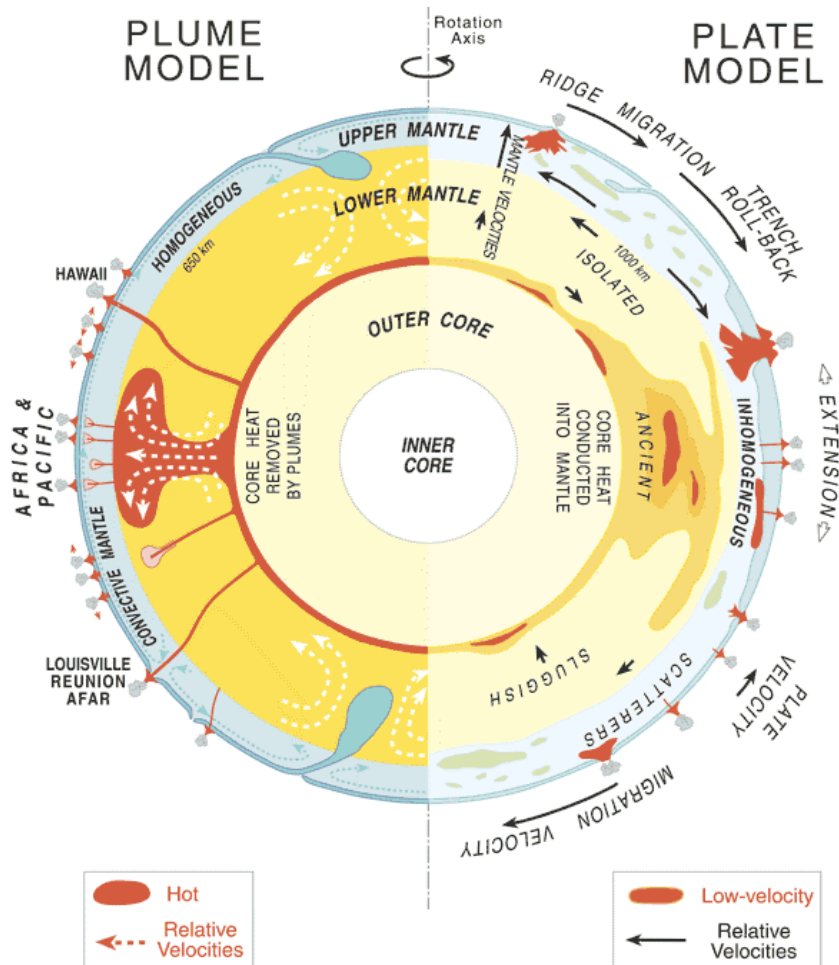


**Figure 1.3.** A schematic cross section of the dynamic earth along its rotational axis. Plume and Plate models of hotspot formation are demonstrated in left and right halves of the earth (after Anderson, 2007).



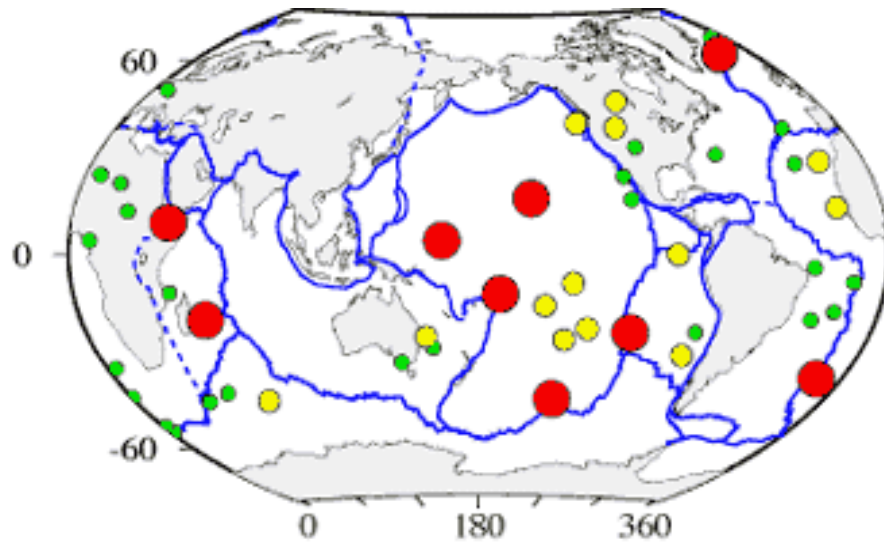


**Figure 1.4** Global distribution of three types of hotspots; Primary and likely to be primary (Red), secondary (yellow) and stress related (green) (after Courtillot et al., 2003).

### **1.3.2 Hotspot Expressions on Lithospheric Plates**

Hotspots originate due to the gravitational instability of a lower thermal layer in the lower mantle and propelled by its own buoyancy and can stuck at any part of the Earth's surface. The interaction between the upwelling magma and oceanic lithosphere produces hotspot features like seamount chains, swells, volcanic islands, underplating, etc. On Earth surface hotspots can exist near or away from the plate boundaries. The Iceland was formed by a hotspot activity on the spreading ridge; this causes excessive thickening of oceanic crust and its elevation above sea surface. The Hawaii hotspot, which had formed the Hawaiian-Emperor island-seamount chain extending about 4000 km from Aleutian Islands to the active Kilauea volcano on the island of Hawaii, is an example of mid-plate volcanism. Hotspots can also form topographic swells of elevation up to 3 km and width up to 1000 km. The swell is parabolic in shape and extent upstream from the active hotspot. The excess elevation associated with the swell decays slowly with the hotspot track. The pacific swell is associated with the Hawaii hotspot.

The hotspot initial eruptions on continental lithosphere, in general, produce volcanic provinces with massive flood basalts. These are interpreted as plume heads marking the initiation of hotspot activity, which in subsequent phases, may leave trace on oceanic crust. The major hotspot related flood basalt provinces are Reunion-Deccan, Iceland-Tertiary North Atlantic, Tristan da Cunha-Parana and Prince Edward-Karoo (Turcotte and Schubert, 2002). Deccan volcanic province provides spectacular evidence for pressure-release melting of Deccan plume head as it impinged on the Indian plate. Within a short span of 1 Myr about  $1.5 \times 10^6 \text{ km}^3$  magma material was pored in to form a large Deccan volcanic province. This volcanism continued approximately for next 65 Myrs, over which the Indian plate moved northward resulting the formation of the Chagos-Laccadive Ridge and Mascarene Ridge, and currently the hotspot is right below the Reunion Island on African plate (White and McKenzie, 1989). The Rajmahal traps present in the eastern part of India is considered as product of the Kerguelen hotspot about 117 Ma, which later formed the Ninetyeast Ridge in the northeastern Indian Ocean (Weis and Frey, 1991).

### **1.3.3 Fixity of Hotspots**

The classical idea of deep anchored hotspot provides a fixed reference system for measuring the absolute plate motions in addition to the relative plate motions. This model has successfully been used to explain the age progressions along the linear volcanic chains. The bend in the hotspot track is explained by the change in direction of plate motion over the fixed hotspot. The sharp bend in the Hawaiian hotspot track between Hawaii and Emperor Islands is a result of abrupt change in the direction of Pacific plate motion over the hotspot. However, the concept of fixed plumes to explain the hotspots activity is currently shaking and not universally accepted. Studies on inter-hotspot movements suggest that the primary hotspots in Pacific and Indo-Atlantic hemispheres currently move very slowly ( $<5$  mm/yr), but in the geological past prior to 50 Ma, they had moved relatively faster (Courtilot et al., 2003). Molnar and Stock (1985, 1987) showed that average velocities between the Hawaiian hotspot and those in the Indo-Atlantic hemisphere for the last 65 Ma have been 10-20 mm/a. In subsequent studies Koppers et al. (2001) argued that motions between certain Pacific hotspots must have reached much higher velocity of more than 60 mm/yr. Later Courtilot et al. (2003) made a significant observation that these higher rates were estimated with the hotspots of specific type (non-primary), but in the case of primary hotspots the analysis could not find evidences for significant inter-hotspot motion greater than 5 mm/yr. This clearly implies that the proposition of fixed hotspot theory is still acceptable for the primary plumes and for other types of hotspots the moments need to be studied in detail.

### **1.4 Aseismic Ridges**

A long linear or broad-plateau like structural highs with a relief of 2 to 3 km lie on the ocean floor, are termed as aseismic ridges. The ridges were emplaced on oceanic crust under various tectonic settings: near or on spreading centre, near to the subduction zones or as isolated features away from plate boundaries. Following the mode of origin, aseismic ridges are classified as volcanic ridges, seamount chains, plateaus, continental fragments, etc. Major aseismic ridges in the global oceans in order of decreasing total volume, are the Ontong-Java Plateau, the Kerguelen Plateau, the Caribbean, the Ninetyeast Ridge, the

Chagos-Laccadive Ridge and the Mid-Pacific Mountains. These six major features constitute 54% of the total crustal volume of all oceanic plateaus of the Earth (Schubert and Sandwell, 1989). A substantial fraction of crustal volume of global oceanic plateaus was subducted and some part was accreted onto the continents, leading to the formation of new continental lithosphere.

Most of the volcanic ridges and seamount chains are formed by the hotspot interaction with the oceanic plates. Confirmation of hotspot origin for the ridges/ seamount chains comes from radiometric dating of basalt samples of the aseismic ridges. The age progression along the aseismic ridges is an important constraint to understand the plate motions over the hotspots. The importance of aseismic ridges in understanding the tectonic histories of lithospheric plates is described in detail in section 1.4.1.

The other type of aseismic ridges are submarine plateaus or rifted pieces of continental blocks. Schubert and Sandwell (1989) have mapped submarine plateaus in world oceans and estimated that submarine continental plateaus accounts about 3.2% of the total continental crustal volume. Significant continental plateaus, in decreasing order of volume, are the Falkland Plateau, the Lord Howe Rise, the Campbell Plateau, the Arctic Ridges, the Mascarene Plateau and the Chatham Rise. These six plateaus constitute 75% of the continental crustal volume on the ocean floor. The age of continental submarine plateaus are generally much greater than the surrounding seafloor age, which generally marks the age when the fragment detached from the parent continent. Some of the submarine plateaus together with the oceanic lithosphere have subducted into the mantle in the past, forming an important route for returning of continental crust to mantle.

#### **1.4.1 Aseismic Ridges- Record of Absolute and Relative Plate Motions**

The kinematic theory of plate tectonics is based upon Euler's theorem, it states that motions on a sphere can be expressed as a rigid rotation about an axis (Cox and Hart, 1986). The motion of any lithospheric plate on the surface of a spherical approximation of the Earth can be described by a rotation about an axis called as Euler pole. The plate motion with

reference to the Euler pole is called finite rotation and these rotations in series are generally used to describe the movement of a lithospheric plate over a period. The plate motions can be relative or absolute: the relative plate motion is described by keeping one plate fixed and moving the other one, whereas absolute plate motion is described with respect to a stationary point deep inside the Earth. If a lithospheric plate moves over a hotspot that is considered as fixed relative to the mantle, the hotspot will create a line of volcanism that follows the trace of a small circle about an Euler pole. This trace of volcanism can then be used to determine the Euler pole and opening angle that describes the plates motion relative to the fixed hotspot i.e., absolute plate motion (APM). Morgan (1971, 1972) was the first to use the geometry and age progressions along the Hawaiian-Emperor, Tuamotu-Line, and the Austral-Gilbert-Marshall chains to develop an absolute plate motion model for the Pacific plate. He used two poles of rotation to describe Pacific APM since 100 Ma with a major change in APM occurring at 43 Ma, reflected by the Hawaiian-Emperor bend.

## **1.5 Concept of Isostasy**

The term “isostasy” is derived from Greek words “iso” and “stasis” meaning “equal standing”. The term is used to describe an equilibrium to which the Earth’s crust and mantle tend, in the absence of disturbing forces (Watts, 2001). Geological processes like volcanism, sedimentation, glacial movements, etc., disturb the equilibrium or static state of the Earth’s outer shells - the crust and mantle. In general, Isostasy explains how Earth’s crust and mantle responds to volcanic loads to maintain its state of equilibrium for a range of spatial and temporal scales. Isostatic observations are important tools to study the Earth’s rheology, composition, structure and dynamics.

The idea of isostasy was first put forwarded by Leonardo Da Vinci in fifteenth century, wherein he had explained the rise of mountain with the removal of materials. However, the development of isostasy further grew in eighteenth century, that was the time scientists have attempted to estimate the mean density and shape of the Earth. One notable contribution has come from the French scientist, Pierre Bouguer, who had attempted to

determine the Earth's mean density by measuring the deflection of the plumb-line (vertical direction) by the mass of a nearby mountain. His experiments ended with contrasting results; the ratio of density of crust to the mean density of the Earth estimated for Mt. Chimborazo in Ecuador, is quite higher than half to that of Mt. Quito in Peru. The erroneous result indicated that the deflection of the vertical caused by the mountain was too small for its estimated mass.

In the first half of the nineteenth century (1806-1843), the English geodesist George Everest carried out triangulation surveys in India. He observed that the distance measured by triangulation between Kalianpur on the Indo-Ganges plain and Kaliana in the foothills of the Himalayas differed substantially from the separation of the sites computed from the elevations of stars (Everest, 1857-59). He opined that that the discrepancy must have caused by errors in geodetic measurements. However, Pratt (1855) attributed the discrepancy to deflection of the plumb-line by the mass of the Himalayas and observed that the minimum deflection of the plumb-line that might be caused by the mass of the Himalayas, is about three times larger than the observed deflection. These observations further lead to a conclusion that the attraction of the mountain range on the plumb-line was not as large as it should have been.

### **1.5.1 Isostatic Compensation Mechanisms**

The plumb-line deflection problem was explained with two contrasting mechanisms by Airy (1855) and Pratt (1855). Both mechanisms suggest local compensation of the extra mass of a mountain above sea-level by a less-dense region (or root) below sea-level, but they differ in the way the compensation is achieved. Hayford (1909) derived a mathematical model to describe the Pratt hypothesis. As a result, this theory of isostasy is often called the Pratt–Hayford scheme of compensation. Whereas, Heiskanen (1931) derived sets of tables for calculating isostatic corrections based on the Airy model. This concept of isostatic compensation has since been referred to as the Airy–Heiskanen scheme. In 1889 C. E. Dutton referred to the compensation of a topographic load by a less-dense subsurface structure as *isostasy*. In the first half of twentieth century Putnam (1912)

and Birell (1914) put forward the idea of regional isostasy, in which the geological loads are supported by the rigidity of the crust. Further, Vening Meinesz worked on these aspects and proposed a third model, in which the crust acts as an elastic plate. As in the other models, the crust floats buoyantly on a substratum, but its inherent rigidity spreads topographic loads over a broader region.

### 1.5.1.1 Airy–Heiskanen Model

Airy–Heiskanen model assumes that the crust is thin and lighter and floats on a thicker and denser substratum like ice bergs floating in water. The height of a mountain above sea-level is much less than the thickness of the crust underneath it, just as the visible tip of an iceberg is much smaller than the subsurface part. The densities of the crust and mantle are assumed to be constant; the thickness of the root-zone varies in proportion to the elevation of the topography. The thickness of continental crust is 30-35 km and the compensation take place below this depth. Oceanic crust is thinner with an average thickness of 6-8 km and the region below forms anti-roots.

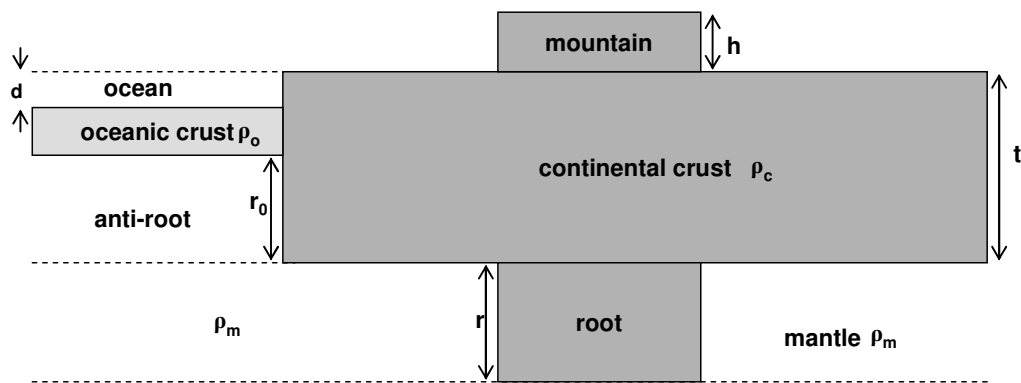


**Figure 1.5** Isostatic compensation according to Airy- Heiskanen model.

According to this model the isostatic compensation is complete and hydrostatically balanced. The thickness of the root zone of a mountain of thickness  $h$  with density  $\rho_c$  (Figure 1.5) is given by (Lowrie, 2007)

$$r = \frac{\rho_c}{\rho_m - \rho_c} * h \quad \dots (1.1)$$

where  $\rho_m$  is the density of mantle. The thickness  $r_o$  of the anti-root of the oceanic crust under an ocean basin of water depth  $d$  and density  $\rho_w$  is given by

$$r_o = \frac{\rho_c - \rho_w}{\rho_m - \rho_c} * d \quad \dots (1.2)$$

### 1.5.1.2 Pratt–Hayford Model

The Pratt–Hayford isostatic model is based on the contraction theory; the depressions and elevations on the Earth's surface are considered as the product of thermal contractions and expansions. This implies that the isostatic compensation is locally attained at a particular depth of compensation by lateral density variations. The elevated regions are underlain by low density rocks whereas depressed regions are underlain by high density rocks.

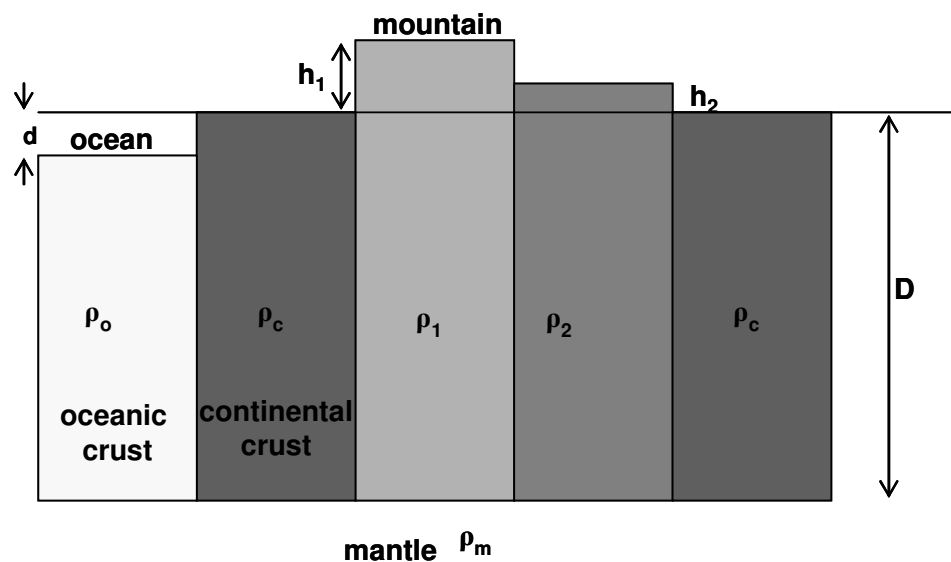


**Figure 1.6** Isostatic compensation according to Pratt–Hayford model

If the rock beneath a mountain of height  $h_i$  ( $i=1, 2, \dots$ ) has density  $\rho_i$ , and if the rock columns are in equilibrium at a depth  $D$  (Figure 1.6), Then the density below a topographic elevation  $h_i$  is given by (Lowrrie, 2007)



$$\rho_i = \frac{D}{h_i + D} * \rho_c \quad \dots(1.3)$$

where  $\rho_c$  is the mean density of the crust. The density under an oceanic basin of depth  $d$  is given by

$$\rho_i = \frac{\rho_c D - \rho_w d}{D - d} \quad \dots(1.4)$$

### 1.5.1.3 Vening Meinesz Elastic Plate Model

The Pratt–Hayford and Airy–Heiskanen models are both idealized with regard to the density distributions and behavior of the Earth’s materials. These models assume that Earth’s upper part offers no resistance to shear stress leading to vertical adjustments between adjacent columns. Like earlier models the Vening Meinesz model also considers a two-layer Earth model, but the upper layer behaves like an elastic plate overlying a weak fluid (Vening Meinesz, 1939). The strength of the plate distributes the load of a surface feature (e.g., an island or seamount) over a horizontal distance wider than the feature (Figure 1.7).

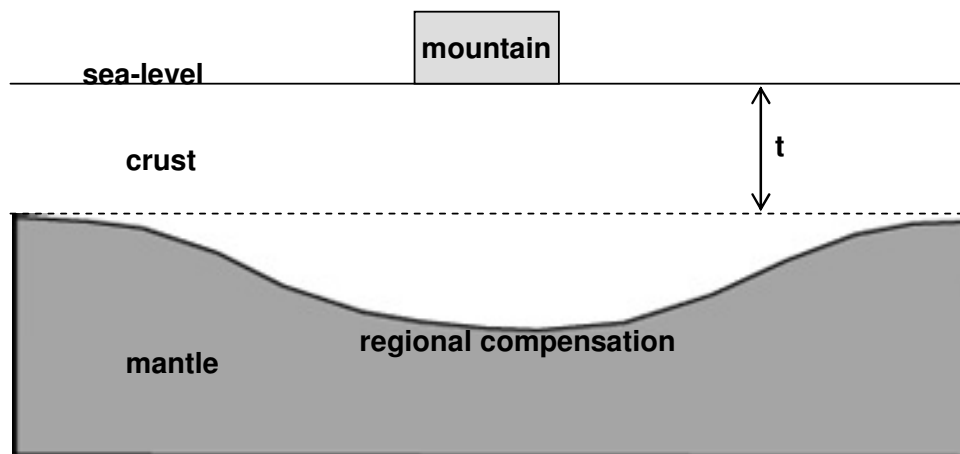


**Figure 1.7** Isostatic compensation according to Vening Meinesz elastic plate model

The topographic load bends the plate downward into the fluid substratum, which is pushed aside. The buoyancy of the displaced fluid forces it upward, giving support to the bent

plate at distances well away from the central depression. The bending of the plate which accounts for the regional compensation in the Vening Meinesz model depends on the elastic properties of the lithosphere.

## 1.6 Elastic Plate Thickness and Flexural Rigidity

The elastic properties of the lithosphere are studied by applying the theory of plate bending in response to applied forces. This model describes the lithosphere as an elastic thin plate that flexes elastically in response to loads. The parameter that characterizes the apparent flexural strength of the lithosphere is the flexural rigidity which is an important factor when parameterizing flexural isostasy. Flexural rigidity is commonly expressed in terms of elastic plate thickness,  $T_e$ , which approximates the Earth's uppermost, elastically deforming layer as a thin elastic plate. If the plate is continuous, homogeneous, and elastic, the flexural rigidity of the plate is defined in terms of Young's modulus  $E$ , the Poisson's ratio  $\nu$  and the effective elastic thickness  $T_e$  with the following equation (Watts, 2001)

$$D = \frac{ET_e^3}{12(1-\nu^2)} \quad \dots(1.5)$$

The deflection of the plate depends on the properties of the plate, or in other words, how resistant is the material of the plate against a deformation. A flexural model where the plate has no strength ( $T_e=0$ ) approximates the classical Airy model for local compensation. The theory of elastic plates and methods of  $T_e$  estimation are described in detail in Chapter 3.

## 1.7 Isostatic Compensation of Aseismic Ridges and Seamounts

Elastic plate model is a simple and powerful tool for understanding the deformation caused by loading and unloading related to various geological processes like post-glacial rebound, mountain orogeny, submarine volcanism, evolution of sedimentary basins etc (Watts, 2001 and references therein). Isostasy and structure of numerous aseismic ridges and seamounts that occur in World's Oceans are studied using flexural modeling (McKenzie and Bowin 1976; Watts 1978; Detrick and Watts 1979; Watts, 1982). They are mainly volcanic in

origin and exist in various tectonic settings. The response of aseismic ridges indicate the long-term mechanical ( $>10^6$  yrs) properties of the oceanic lithosphere, which are expressed in terms of the effective elastic thickness. The value of  $T_e$  depends on mineralogy, temperature, and state of stress of the lithosphere. Oceanic lithosphere, with a thin and mafic crust, generally behaves like a single mechanical layer. Oceanic mantle is relatively homogeneous, and the ocean geotherm is dominated by plate cooling, so  $T_e$  of oceanic lithosphere increases with thermal age of the lithosphere at the time of loading (Watts, 1978). This important property of the  $T_e$  has been used to date aseismic ridges and to infer the tectonic setting of its origin. Further details of  $T_e$ -age relation and its tectonic interpretation are discussed in Chapters 4, 5 and 6.

## 1.8 Objectives

The present work consists of a detailed geophysical study of the structure and isostatic compensation mechanisms of three major aseismic ridges; The Comorin Ridge, The 85°E Ridge and Ninetyeast Ridge of the northeastern Indian Ocean. The major objectives of the study are

### 1. The Comorin Ridge

- a) to determine the elastic plate thickness ( $T_e$ ), crustal thickness and isostatic compensation mechanism of the Comorin Ridge
- b) to demarcate the Continent-Ocean Boundary (COB) on the southwest margin of Sri Lanka and southern tip of India
- c) to outline the tectonic setting of the ridge

### 2. The 85°E Ridge

- a) to develop a process oriented modeling technique for determining the elastic plate thickness of the ridge
- b) to determine the crustal structure and isostatic compensation mechanism of the ridge

- c) to investigate the changes in ridge gravity anomaly through time since its formation and discuss the geological processes.

### **3. The Ninetyeast Ridge**

- a) to study the variation in elastic plate thickness along Ninetyeast Ridge using admittance analysis and forward model techniques
- b) to determine crustal structure and isostatic compensation mechanism of the ridge.
- c) to discuss the spatial variations in the  $T_e$  in the light of complex interactions between the Kerguelen hotspot and oceanic lithosphere.